

Article

Detection and crystal structure of hydrogenated bipentacene as an intermediate in thermally-induced pentacene oligomerization

Craig I. Hiley, George F. S. Whitehead, Marco Zanella, Charlene Delacotte, Troy D. Manning, and Matthew J. Rosseinsky

J. Org. Chem., **Just Accepted Manuscript** • DOI: 10.1021/acs.joc.9b00671 • Publication Date (Web): 04 Jun 2019

Downloaded from <http://pubs.acs.org> on June 10, 2019

Just Accepted

“Just Accepted” manuscripts have been peer-reviewed and accepted for publication. They are posted online prior to technical editing, formatting for publication and author proofing. The American Chemical Society provides “Just Accepted” as a service to the research community to expedite the dissemination of scientific material as soon as possible after acceptance. “Just Accepted” manuscripts appear in full in PDF format accompanied by an HTML abstract. “Just Accepted” manuscripts have been fully peer reviewed, but should not be considered the official version of record. They are citable by the Digital Object Identifier (DOI®). “Just Accepted” is an optional service offered to authors. Therefore, the “Just Accepted” Web site may not include all articles that will be published in the journal. After a manuscript is technically edited and formatted, it will be removed from the “Just Accepted” Web site and published as an ASAP article. Note that technical editing may introduce minor changes to the manuscript text and/or graphics which could affect content, and all legal disclaimers and ethical guidelines that apply to the journal pertain. ACS cannot be held responsible for errors or consequences arising from the use of information contained in these “Just Accepted” manuscripts.

Detection and crystal structure of hydrogenated bipentacene as an intermediate in thermally-induced pentacene oligomerization.

Craig I. Hiley, George F. S. Whitehead,[†] Marco Zanella, Charlene Delacotte, Troy D. Manning, Matthew J. Rosseinsky*

Department of Chemistry, University of Liverpool, 51 Oxford Street, Liverpool, L7 3NY

*Corresponding author m.j.rosseinsky@liverpool.ac.uk

[†]Current address: University of Manchester, School of Chemistry, Oxford Road, Manchester, M13 9PL

Abstract

6,6',13,13'- tetrahydro-6,6'-bipentacene (**HBP**), the intermediate molecule connecting pentacene to previously observed peripentacene and extended pentacene oligomers through the formation of a carbon-carbon bond, is synthesised and crystallographically characterised. Heating pentacene to 300 °C under vacuum for 200 hours results in pale golden crystals of **HBP** and amorphous material containing pentacene oligomers, offering experimental evidence that pentacene preferentially dimerizes at the 6,6'-position. Continued heating of **HBP** results in co-crystals of 6,13-dihydrogenated pentacene (**HP**) and pentacene and further amorphous pentacene oligomers. The amorphous material consists of layered carbonaceous species with a graphenic nature, as determined by Raman spectroscopy and electron microscopy, and suggests **HBP** as an intermediate to hydrogenated pentacene species and pentacene oligomers, such as peripentacene, of interest in organic electronics.

Introduction

Conjugated small organic molecules have been the focus of intense research for use in organic electronic devices due to high charge mobility, mechanical flexibility and low cost (compared to typical inorganic compounds).^{1,2} Pentacene, consisting of five linearly-fused aromatic rings (**P**, Figure 1a), has generated more interest than any other conjugated molecule for use in these devices thanks to its particularly high conductivity and the availability of a range of deposition techniques leading to uniform highly-ordered thin films.^{1,3} When making thin films, the most widely-employed technique is vacuum deposition, not least because it can be considered a simultaneous purification step.³ This technique typically involves high temperature and low pressure to increase the **P** partial pressure. Roberson *et al.*⁴ showed that under an inert gas flow at 320 °C, in competition with its sublimation, **P** disproportionates to give a 2:1 co-crystal of 6,13-dihydrogenated pentacene (**HP**, Figure 1a) and **P**,⁵ and peripentacene (**PP**, Figure 1a), detected by mass spectrometry. **PP** can be considered as two pentacene molecules completely fused along one long axis and has been described as a graphene fragment.^{6,7} The mechanism for this transformation in the solid state is a matter of some debate,^{4,8} and since the initial report of **PP**, considerable effort has gone into developing a rational route to its synthesis.^{6,9} Thermolysis of a variety

1
2
3 of other acenes has been demonstrated to drive both intramolecular C–C bonding^{10,11} and intermolecular
4 addition reactions to form oligomeric¹² and graphitic species.¹³ Recently Rogers *et al.*⁶ succeeded in
5 preparing single molecules of **PP** on an Au surface via the dehydrogenation of 6,6'-bipentacene (**BP**,
6 itself chemically synthesised in bulk from functionalised pentacene derivatives⁶), which *ab initio*
7 calculation⁴ proposes as an intermediate in **PP** formation in the solid state. Subsequent calculations⁸
8 showed that the mechanism is likely to be initiated when a 6-hydropentacenyl radical (**HPR**, Figure 1a)
9 – formed by the hydrogen atom transfer from catalytic amounts of **HP** to **P** – dimerizes to give the
10 intermediate species 6,6',13,13'-tetrahydro-6,6'-bipentacene (**HBP**, Figure 1a), or adds to a **P** molecule
11 to form a dimer radical. Either **HBP** or the dimer radical can be transformed to **PP** by a series of H
12 abstractions by **P** or **HPR** species to generate significant quantities of **HP**. To date, no experimental
13 reports of formation of any intermediate dimers (**BP** or **HBP**) through C-C bond formation upon heating
14 solid pentacene have been published and their status as intermediates in the thermal formation of **PP**
15 remains unclear. The evidence for the existence of **PP** is mass spectrometry, which may be identifying
16 only the most volatile components of the bulk material, and Raman spectroscopy,¹⁴ for which the
17 features are common to all sp² carbon phases. By heating at the slightly lower reaction temperature of
18 300 °C under vacuum and studying the resulting materials with a range of bulk characterisation
19 methods, we demonstrate the transformation of as-received pentacene to a mixture of single crystalline
20 **HBP** and a carbon-rich amorphous phase (Figure 1c), likely to be composed of oligomerised pentacene.
21 This represents experimental evidence for preferential intermolecular C–C bond formation at the 6, 6'
22 positions in the thermal oligomerisation of pentacene, yielding a crystallographically-characterised
23 pentacene oligomer by solid-state thermal transformation. **HBP** is shown to be unstable, and upon
24 further heating it is further transformed to give the previously reported **2HP:P** co-crystals and additional
25 amorphous oligomerised pentacene as formed in the first heating step. The transformation of **HBP** to
26 **2HP:P** co-crystal and amorphous material demonstrates the importance of **HBP** as an intermediate
27 compound in the thermally-driven formation of pentacene-based oligomers, and hydrogenated
28 pentacene. The amorphous material has been shown to consist of thin, extended sheets which can be
29 readily exfoliated, suggesting this material may be 'graphenic' in nature.
30
31
32
33
34
35
36
37
38
39
40
41
42
43
44
45
46
47
48
49
50
51
52
53
54
55
56
57
58
59
60

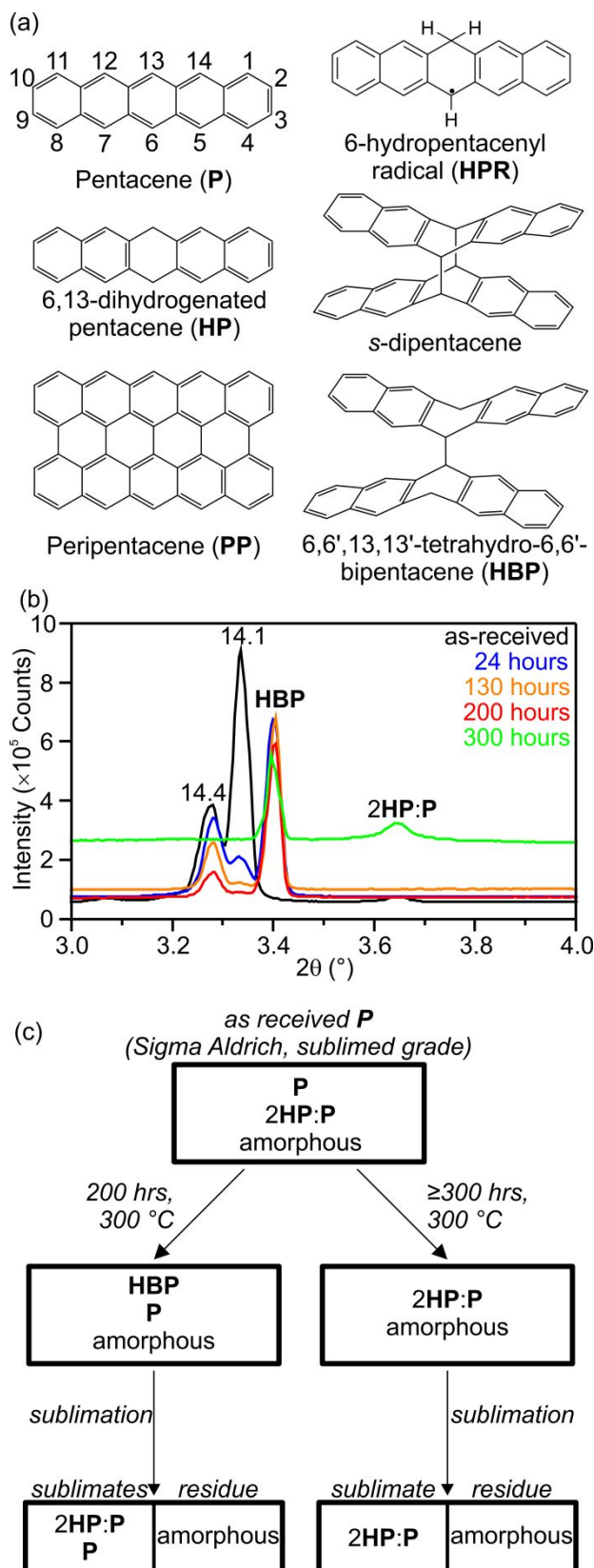


Figure 1. (a) Pentacene (with carbon positions numbered) and related derivatives relevant to its thermal reactivity. (b) SXRDR patterns of pentacene heated at 300 °C for 0 – 300 hours, showing the peaks arising from polymorphs of pentacene (so called ‘14.1 Å’ and ‘14.4 Å’ polymorphs), **HBP** and **2HP:P** co-crystals. (c) Scheme of observed products from heating of as-received pentacene.

Results and Discussion

Figure 2b shows the synchrotron powder X-ray diffraction (SXR) pattern of as-received pentacene (Sigma Aldrich, sublimed grade >99.9% trace metals basis). Fitting to this pattern shows that it contains a mixture of the two known bulk-phase polymorphs,^{3,15-18} but also a significant proportion (12.3(2)% by mass, Table S2) of **2HP:P** co-crystals, where **HP** has been previously suggested as a likely catalyst in pentacene disproportionation.⁸ 50 mg of this as-received pentacene powder was pelletized and sealed in a Pyrex tube evacuated to 2×10^{-5} mbar. Upon heating at 300 °C for 24 hours pale, golden-coloured crystals were observed on the surface of the black pellet. Single crystal X-ray diffraction confirms the identity of these crystals as the previously undetected **HBP** (Figure 2a, Figure S3). The unit cell (space group $P2_1/n$, Figure S4) contains just one 6'-hydropentacenyl subunit within the asymmetric unit, with a centre of inversion at the centre of the dimer molecule. The C–C bond between the two 6-hydropentacenyl subunits forms between the 6 and 6' carbons, yielding the isomer calculated to be the most energetically favoured.⁸ This bond is notably long at 1.601(2) Å (at 150(2) K); ~0.1 Å longer than a typical C–C bond. This can be thought of as arising from quadrupolar repulsion of the neighbouring aromatic systems with C...C distances of as little as 3.166(2) Å between the 5 and 5' (and 7 and 7') positions, Figure 2a). Similar bond lengths are also observed in 'sandwich photodimers' of acenes,¹⁹⁻²¹ whereby two new C–C bonds form between two parallel stacked acene subunits across an aromatic ring overlapping π systems. For example, in *s*-dipentacene²¹ (Figure 1a) C–C bonds form between the 6:6' and 13:13' positions with a mean bond length of 1.611(2) Å, leading to $\pi \cdots \pi$ interactions between the closest aromatic rings of mean distance 3.885(3) Å (as measured from the aromatic centroids), close to the ideal distance for $\pi \cdots \pi$ stacking.²² Note this is significantly longer than the C5–C5' distance in **HBP**, due to larger bond angle around the sp^3 carbon atoms in the sandwich dimer (~112.5°, compared to ~109° in **HBP**). In **HBP** there is only one C–C bond between the subunits, and the resulting 'stepped' configuration minimises quadrupolar repulsion within the molecule. Raman spectroscopy of a **HBP** (point group C_{2h}) single crystal (Figure 3a) shows sharp peaks at 790 cm^{-1} , 834 cm^{-1} , 931 cm^{-1} , 1017 cm^{-1} , 1387 cm^{-1} , 1469 cm^{-1} and is used as a fingerprint for the identification of **HBP** in the Raman spectra of bulk samples.

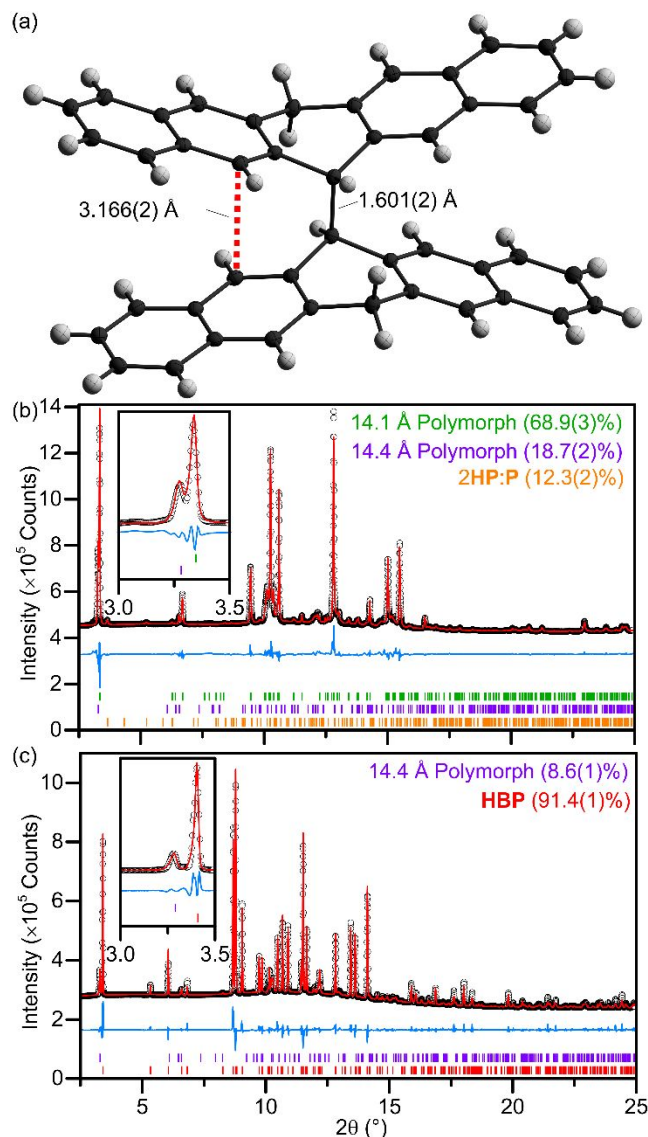
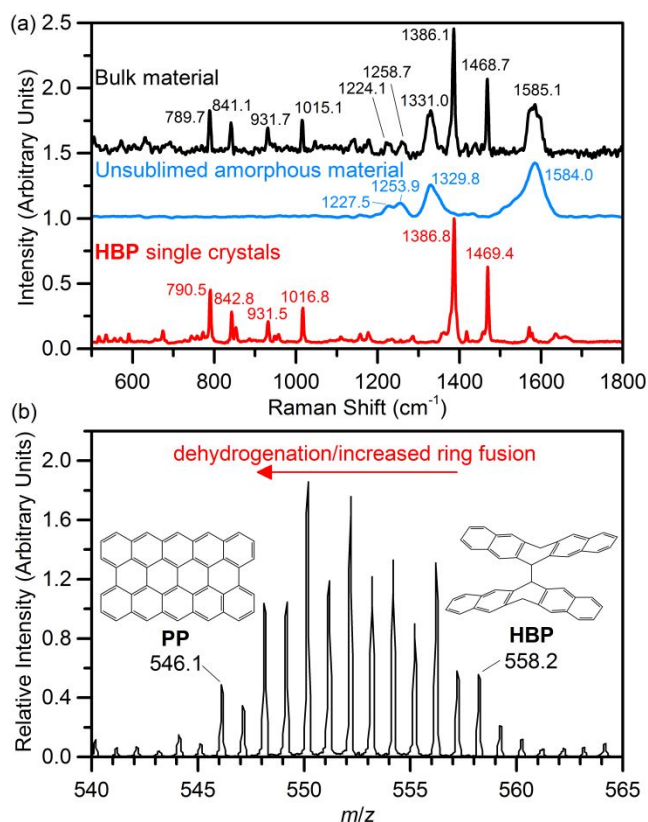


Figure 2. (a) Refined structure of **HBP** from single crystal X-ray refinement (data measured at 150(2) K) with thermal ellipsoids at 50% probability. (b) SXR D of as-received Sigma Aldrich pentacene with multi-phase Rietveld refinement of two pentacene polymorphs^{3,16} and 2HP:P co-crystals.⁵ $R_{wp} = 5.03\%$. Inset shows partially resolved (001) peaks of both pentacene polymorphs. (c) SXR D of pentacene after heating *in vacuo* at 300 °C for 200 hours, with multi-phase Rietveld refinement of **HBP** with a residual amount of pentacene. $R_{wp} = 4.48\%$. Full details of refinements in Tables S2 and S3.

The pellet of **P** treated at 300 °C for 24 hours was ground into a fine powder and SXR D (Figures 1b, S5) shows that a majority of the **P** is converted to **HBP**. Optimisation of the synthesis time found that heating at 300 °C for 200 hours yields a sample where > 90% (by mass) of the crystalline component was **HBP**, with **P** comprising the remainder of the crystalline portion (Figure 2c, Table S3). Despite this high degree of conversion, the pellet remains a black colour, inconsistent with the observed pale colour of the single crystals of **HBP**, suggesting the presence of a secondary amorphous phase. Raman spectroscopy confirms the presence of the secondary amorphous phase by comparison of the bulk

material and single crystals of **HBP** extracted from the surface of the pellet (Figure 3a). The Raman spectra show four broad peaks ($\nu = 1224 \text{ cm}^{-1}$, 1259 cm^{-1} , 1331 cm^{-1} and 1585 cm^{-1}) present in the bulk material in addition to peaks assigned to **HBP**. Elemental analyses of as-received pentacene gave a measured C:H mass ratio of 18.9 and the mixture of **HBP** and amorphous material produced by the thermal treatment show the same measured C:H mass ratio (18.8), and since **HBP** is hydrogenated with respect to pentacene (theoretical C:H mass ratio for **HBP** is 17.5), the amorphous material is assumed to be carbon-rich with respect to the starting material. Quantification of the amorphous component by SXRD using an internal standard (monocrystalline diamond powder, Sigma Aldrich) shows the sample contains approximately one-third (by mass) amorphous material (Figure S6, Table S4). This is a larger amorphous contribution than would be expected if **PP** were the only component of the amorphous phase (~17%). For comparison, as-received pentacene was found by the same method to contain ~10% amorphous material. An attempt to separate **HBP** from the amorphous material by heating the mixture to $300 \text{ }^\circ\text{C}$ at the end of a sealed evacuated tube with the opposing end of the tube at room temperature (Figure S1) led to the decomposition of **HBP**, resulting in sublimation of only yellow and purple–red **2HP:P** co-crystals and a small quantity of unreacted pentacene. Subsequent powder SXRD of the residual post-sublimed material showed no crystalline peaks, confirming that **HBP** is unstable over extended heating periods and decomposes to form hydrogenated pentacene species and amorphous material.



1
2
3 **Figure 3.** (a) Raman spectra (exciting laser $\lambda = 785$ nm) of single crystals of **HBP**, residual post-sublimed
4 amorphous material and the bulk mixture of **HBP** and amorphous material. (b) High resolution EI-MS data of
5 residual post-sublimed amorphous material. Full MS spectrum ($50 \leq m/z \leq 900$) shown in Figure S9.
6
7

8 Heating pentacene at 300 °C for the longer time of 300 hours leads to formation of a product consisting
9 of **2HP:P** co-crystals and amorphous material (Figures 1b, S5) with a small quantity of **HBP** remaining,
10 suggesting that **HBP** initially formed in the reaction is transformed over the extended heating period.
11 The transient nature of **HBP** is the most likely explanation for the difficulty in observing it in earlier
12 experiments.⁴ Sublimation of the mixture of **2HP:P** co-crystal and amorphous material, as described
13 above for the **HBP**/amorphous mixture, resulted in **2HP:P** co-crystals at the cool end of the tube, with
14 a significant proportion of residual post-sublimed black material remaining which was further
15 characterised to determine the nature of any oligerimized pentacene products potentially formed during
16 the annealing of sublimed pentacene thin films for use in organic electronics as discussed in the
17 introduction. The black material is completely amorphous by SXRD (Figure S7), and the Raman
18 spectrum (Figure 3a), an effective probe of carbonaceous structure,²³⁻²⁷ consists of only 4 peaks at
19 1228 cm^{-1} , 1254 cm^{-1} , 1330 cm^{-1} and 1584 cm^{-1} , coinciding with the peaks of the secondary phase
20 observed in the Raman spectrum of the as-made mixture of **HBP** and amorphous material (Figure 3a),
21 suggesting that this amorphous material is formed concurrently with **HBP** and is unchanged by further
22 heating. The spectrum agrees broadly with both the calculated Raman spectrum for **PP** and the observed
23 spectra of pentacene samples heated under vacuum at higher temperatures (425 °C – 800 °C).¹⁴
24 However, the two strongest peaks, at 1584 cm^{-1} and 1330 cm^{-1} , can also be assigned to the *G* (resulting
25 from in-plane optic phonons) and *D* (caused by structural defects) modes of extended sp^2 carbon
26 structures, such as graphene and carbon nanotubes, respectively. The high ratio of intensities $I_{(D)}:I_{(G)}$
27 and the lack of any observed second-order modes (>2000 cm^{-1} , Figure S8) would suggest a high degree
28 of disorder,^{24,27-29} consistent with a material containing a distribution of pentacene oligomers, including
29 **PP**, or an extended, partially hydrogenated graphitic material, or graphene nanoribbons, which could
30 be formed by extensive oligomerization. Recently graphene nanoribbons have been shown to exhibit
31 weak phonon modes in the range of 1200-1300 cm^{-1} , which were ascribed to breathing modes of six-
32 atom rings³⁰ and which closely resemble features seen in the Raman spectrum of the amorphous material
33 at 1228 cm^{-1} and 1254 cm^{-1} (Figure 3a). Elemental analysis of the residual post-sublimed amorphous
34 material showed an increased C:H mass ratio (21.9) over the starting pentacene (18.9, consistent with
35 the sublimation of **2HP:P** co-crystals), but still significantly lower than expected for pure **PP**
36 (theoretical C:H mass ratio of 29.1), suggesting only partial fusion or a mixture of products. Sampling
37 by gas chromatography (GC) of the gas in the sealed Pyrex tube after reaction (Figure S2) shows no
38 significant quantity of H_2 gas is evolved at any stage (corresponding to $\ll 1\%$ of the total number of H
39 atoms in the starting material; Figure S10, Table S5). This suggests that fusion under vacuum is not
40
41
42
43
44
45
46
47
48
49
50
51
52
53
54
55
56
57
58
59
60

1
2
3 generating gaseous H₂ as previously proposed,¹⁴ but is driven by H atom transfers to **P** or **HPR**,
4 calculated to be a much lower-energy process.⁸
5
6

7 In previous work, mass-spectrometry (MS) data have offered the most definitive evidence for the
8 presence of **PP**.⁴ High resolution electron ionisation MS (EI-MS) data from the residual post-sublimed
9 amorphous material in the mass range for dimeric pentacenyl species (Figure 3b), show that the sample
10 contains a spectrum of *m/z* values from 546.1 to 558.2, coinciding with masses of **PP** and **HBP**,
11 respectively. A similar distribution of *m/z* values was seen in previous work,⁴ and was ascribed by the
12 authors to partial fusion of the pentacene monomers and/or a misalignment of the pentacene subunits.
13 Based on the computed high favourability of 6,6'-dimerization of **HPR** over formation of other adducts,⁸
14 and our experimental observation of **HBP** as the only (crystalline) intermediate, we assign this
15 distribution of masses to partial fusion and hydrogenation, rather than significant occurrence of
16 misaligned monomers. There is also another cluster of *m/z* peaks between 818.2 and 834.4 (Figure S9),
17 corresponding to the mass range of trimeric, partially dehydrogenated pentacene species (the trimeric
18 analogues of **PP** and **HBP** have masses of 814.2 and 836.3, respectively), demonstrating the ability of
19 the system to further oligomerize. Higher mass oligomers were not observed, but it is unclear whether
20 this is due to their low abundance or poor volatility.
21
22
23
24
25
26
27
28
29

30 Scanning electron microscopy (SEM) of the residual post-sublimed amorphous material suggests that
31 it is composed of thin layers (Figure 4a, b, Figure S11), consistent with an extended sp² material. A
32 suspension of the material in N-methyl-2-pyrrolidone (NMP), a common solvent used in the exfoliation
33 of graphene sheets,³¹ was generated by sonication for 35 hours. After sonication the suspensions have
34 a dark-brown/black colour which is retained for (at least) several months. A droplet of the sonicated
35 suspension was deposited onto a glass slide and the solvent allowed to evaporate. Optical microscopy
36 reveals the presence of sheets up to 200 μm across (Figure 4c), the Raman spectra of which (collected
37 at multiple locations to confirm homogeneity) have modes at the same frequencies as observed in the
38 bulk material (Figure S12). TEM and SEM (Figure 4, Figure S13) show the presence of layers in the
39 material but their thickness was difficult to quantify. For comparison, pristine pentacene in NMP was
40 also sonicated, yielding a suspension which rapidly (<5 minutes) settles to give a black powder and
41 yellow solution of 6,13-pentacenequinone formed by oxidation of pentacene.³² Immediately after
42 sonication, a droplet of the suspension was deposited onto a glass slide. After the NMP evaporated,
43 optical microscopy shows only small black crystals of pentacene and their agglomerates can be
44 observed with no indication of extended sheets forming (Figure S14).
45
46
47
48
49
50
51
52
53
54
55
56
57
58
59
60

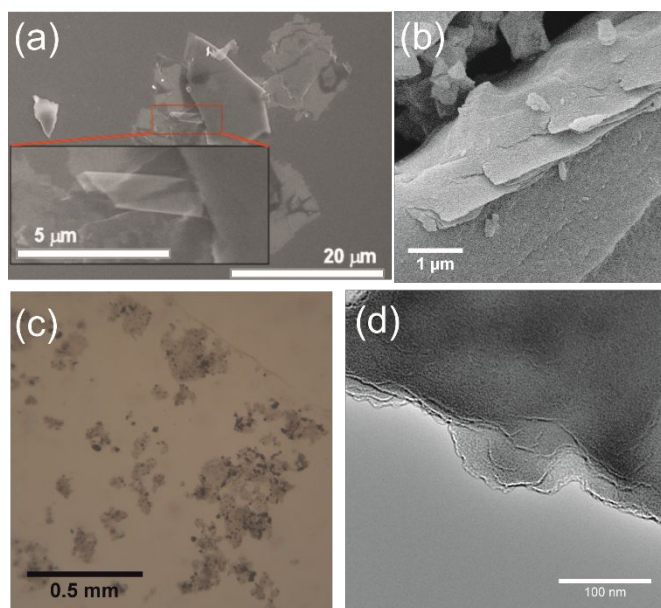


Figure 4. (a) SEM of the bulk amorphous residue material after sublimation of **HBP/2HP:P**, zoomed area shows a single layer exfoliated from the bulk material (b) SEM of bulk residual post-sublimed amorphous material at high magnification showing the layered structure (c) Optical microscopy and (d) TEM of exfoliated residual post-sublimed amorphous material.

Conclusions

We have shown that the previously unobserved dimer **HBP** forms readily upon heating samples of pentacene containing trace amounts of **HP**. The observation of **HBP** represents the first crystallographic characterisation of a C-C bond between pentacene units on the path to extended sp^2 C-C based species. **HBP** is unstable and upon further heating is easily cracked to give **2HP:P** co-crystals and an amorphous by-product, consisting of oligomerized pentacene species at various stages of fusion. Whilst previous work⁴ has suggested that **PP** is the main constituent of this amorphous material, high resolution mass spectrometry data we present suggest that dimeric and higher-order oligomers with various degrees of fusion are also present. Further characterisation of this amorphous mixture indicates partially-hydrogenated graphitic or graphene-like constituents may be present, formed by extensive oligomerization of pentacene which are not detectable by mass spectrometry due to low volatility or fragmentation. No H_2 gas is observed in the reaction vessel at any stage, suggesting that fusion occurs by a series of H-transfer steps. The results confirm the theoretical predictions⁸ that 6-6' fusion is strongly preferred and that formation of isolatable **HBP** is the first step in pentacene oligomerization, providing a starting point for future experimental mechanistic studies. Reliable synthesis of **HBP** offers a useful starting material in the rational synthesis of **PP** and nanographene.

Experimental Section

a) Pentacene Thermolysis

1
2
3 50 mg of as-received pentacene (Sigma Aldrich, sublimed grade, >99.9% trace metals basis) was
4 pressed into a 5 mm diameter pellet under a pressure of 1 ton in an Ar-filled glovebox (with measured
5 levels of O₂ and H₂O <1ppm). The pellet was then placed into a Pyrex tube (outer diameter ~9.5 mm,
6 inner diameter ~5.5 mm), which was subsequently evacuated to a pressure of 2 × 10⁻⁵ mbar. The Pyrex
7 tube was then sealed at a length of 10 – 12 cm and placed in a fan-assisted oven at room temperature.
8 The oven was then heated to 300 °C at a heating rate of 5 °C min⁻¹. After heating for 24 – 300 hours,
9 the oven was cooled to room temperature at a cooling rate of -5 °C min⁻¹.
10

11 Heating at slightly lower temperatures (280 – 290 °C) yields the same reaction, albeit at a much reduced
12 rate, necessitating heating times of over 1000 hours to achieve maximum conversion from pentacene to
13 **HBP**. Single crystals of **HBP** could then be isolated by manual separation (Raman 1469.4, 1386.8,
14 1016.8, 931.5, 842.8, 790.5 cm⁻¹). Heating pentacene at 320 °C failed to isolate **HBP**, instead a mixture
15 containing only amorphous material and **2HP:P** co-crystals were produced.
16
17

18 b) Sublimation

19 A subsequent sublimation step was used to separate crystalline, hydrogenated products from the
20 amorphous, hydrogen-poor material which exhibits low volatility. The mixture was ground into a fine
21 powder using a pestle and mortar and loaded into narrow Pyrex tube (outer diameter ~5 mm, inner
22 diameter ~3 mm, length ~6 cm), which was then itself loaded into a Pyrex tube (outer diameter
23 ~9.5 mm, inner diameter ~5.5 mm). The tube was then evacuated to 2 × 10⁻⁵ mbar and sealed at a length
24 of ~30 cm. The tube was then placed in a three-zone tube furnace such that the sample was at the centre
25 of the furnace and the opposing end was at room temperature (Figure S1a). The centre of the furnace
26 was heated to 300 °C at a heating rate of 5 °C min⁻¹. A thermocouple was used to determine the
27 temperature profile along the length of the tube furnace (Figure S1b), which shows a gradient from 300
28 °C at the centre to 120 °C at the edge of the furnace. After 18 hours the furnace was cooled at a rate of
29 5 °C min⁻¹ to room temperature. After heating, crystals of **P** and **2HP:P** co-crystals were found to be
30 sublimed at the cool end of the tube (Figure S1c).
31
32
33
34
35
36
37
38
39
40
41
42
43
44
45

46 c) X-ray diffraction

47 Single crystal XRD data for **HBP** were collected using a Rigaku MicroMaxTM-007 HF with a
48 molybdenum rotating anode microfocus source and a Saturn 724+ detector. The structure was solved
49 and refined using SHELX-2013.²² Hydrogen atoms were placed in calculated positions using built-in
50 SHELX riding models and assigned isotropic thermal parameters 1.2 times those of their parent atoms.
51 Full crystallographic details are included in Table S1. The supplementary crystallographic data for **HBP**
52 can be obtained free of charge from the Cambridge Crystallographic Data Centre via
53 www.ccdc.cam.ac.uk/data_request/cif, CCDC identifier 1811701.
54
55
56
57
58
59
60

Powder XRD and synchrotron powder X-ray diffraction (SXRD) data were collected at room temperature in transmission mode from 0.7 mm borosilicate capillaries. Laboratory XRD data were collected from a Bruker-AXS D8 Advance diffractometer with a fine focus Mo $K\alpha$ source ($\lambda = 0.71073 \text{ \AA}$), whilst SXRD data were collected at Beamline I11 at Diamond Light Source, UK ($\lambda = 0.82602(1) \text{ \AA}$) using Mythen PSD detectors.

Rietveld refinements were carried out using TOPAS Academic v5.¹ Starting models were either taken from structures reported in literature or (in the case of the new compound HBP) obtained from single crystal XRD. For the Rietveld refinements lattice parameters and a single C constrained thermal displacement parameter were the only structural parameters allowed to refine.

To calculate the amorphous content of HBP/amorphous mixture and pristine pentacene, the sample (20 mg) was ground and thoroughly mixed with a known quantity of monocrystalline diamond powder. A sample of this mixture was then loaded into a 0.7 mm borosilicate capillary for SXRD. Collected SXRD patterns were fitted to multiphase models yielding the ratio of crystalline sample mass: internal standard mass. By comparison to the ratio of total sample mass: internal standard mass, the proportion of the sample that is crystalline (and thus amorphous) is determined (Table S4).

$$\text{Crystalline fraction (by mass)}: \frac{\text{Ratio of crystalline sample mass : internal standard mass}}{\text{Ratio of total sample mass : internal standard mass}}$$

d) Other Characterisation Techniques

Raman spectroscopy was collected using a Renishaw inVia Raman Spectrometer with an excitation laser wavelength of 785 nm.

Elemental analysis for C and H content was performed using a Thermo EA1112 Flash CHNS-O Analyser.

Gas chromatography (GC) to detect any hydrogen emission from the sample was carried out using an Agilent 6890N with He as the carrier gas. After reaction at 300 °C, the circumference of the sealed Pyrex reaction tube was scored at its centre and PTFE washers were placed around the top and bottom. This was then placed in a custom-made break-seal apparatus (Figure S2) adapted from an earlier design by Caldwell *et al.*,³³ inside an Ar filled glove box (O_2 and H_2O levels <1 ppm). The ground glass joint was sealed with a SubaSeal[®] septum. The greaseless stopcock was turned to exert a force on the Pyrex tube at the score mark until it was opened. After 1 minute (to allow the gas to equilibrate), a needle was used to collect a 500 μL sample of the gas, which was injected into the GC. The gas evolved from 50 mg samples of pentacene heated at 300 °C for 200 hours (*i.e.* at maximum conversion to **HBP** and amorphous oligomerised material) and 450 hours (*i.e.* after formation and subsequent decomposition of

intermediate **HBP** to **2HP:P** co-crystals and further amorphous oligomerised material) was measured. In addition, the H₂ levels from an empty tube and 50 mg picene (an isomer of pentacene consisting of zig-zag (rather than linearly) fused aromatic rings that is not susceptible to reaction), both heated at 300 °C for 200 hours were measured. The GC was calibrated to allow quantification using a reference gas of accurately known concentration (500 ppm), which determined a sensitivity of $7(2) \times 10^{-9}$ mg_H per unit area of the H₂ peak. Approximation of the total volume of the break-seal apparatus allowed an estimate of total H₂ gas inside to be calculated.

Electron ionised mass spectrometry was conducted at the EPSRC UK National Mass Spectrometry Facility using a Thermo Scientific DSQ-II.

Exfoliation of the amorphous material was conducted using sonication. 2-3 mg of the amorphous material was added to 0.5 ml of N-methyl-2-pyrrolidone (**NMP**) in a 2 ml vial. The vial was then sonicated for 3 hours to form a suspension that remains stable for (at least) several weeks. A drop of this suspension was deposited onto either a glass slide (for optical microscopy) or a bare (*i.e.* no carbon support) 400 mesh nickel TEM grid (for TEM). The sample was left open to the air for at least an hour to allow solvent evaporation.

Scanning electron microscopy (SEM) was carried out using a Hitachi S-4800 Field-Emission SEM using an accelerating voltage of either 3 kV (for imaging sonicated material suspended on TEM grid) or 10 kV, to collect images of the bulk amorphous material, for which a small amount of powder was spread onto carbon tape and sputter-coated with gold.

Transmission electron microscopy (TEM) was carried out using a 300 kV JEOL 3010.

Optical microscopy was carried out using a Meiji MT9430 microscope.

Acknowledgements: Ms Verity Piercy and Dr Alex Cowan are thanked for assistance with GC measurements. Prof Paul Chalker and Prof Laurence Hardwick are thanked for useful discussions on the Raman spectroscopy of carbonaceous materials, Prof Laurence Hardwick is also thanked for the use of the Renishaw inVia Raman Spectrometer. This work was carried out with the support of the Diamond Light Source on Beamline I11. We are grateful to the EPSRC UK National Mass Spectrometry Facility at Swansea University (Dr Ann Hunter). The work was funded through EPSRC grants EP/K027212/1 and EP/K027255/2.

ASSOCIATED CONTENT

The Supporting Information is available free of charge on the [ACS Publications website](#).

Additional experimental details: sublimation set up, **HBP** crystallographic details, powder synchrotron X-ray diffraction data, additional Raman spectroscopy data, additional mass spectrometry data, gas chromatography data, optical and electron microscopy. Underlying data is available at <http://dx.doi.org/10.17638/datacat.liverpool.ac.uk/445>

References

- (1) Dimitrakopoulos, C. D.; Malenfant, P. R. L., Organic Thin Film Transistors for Large Area Electronics. *Adv. Mater.*, **2002**, *14*, 99-117.
- (2) Garnier, F., Thin-film transistors based on organic conjugated semiconductors. *Chem. Phys.*, **1998**, *227*, 253-262.
- (3) Kitamura, M.; Arakawa, Y., Pentacene-based organic field-effect transistors. *J. Phys.: Condens. Matter*, **2008**, *20*, 184011.
- (4) Roberson, L. B.; Kowalik, J.; Tolbert, L. M.; Kloc, C.; Zeis, R.; Chi, X.; Fleming, R.; Wilkins, C., Pentacene Disproportionation during Sublimation for Field-Effect Transistors. *J. Am. Chem. Soc.*, **2005**, *127*, 3069-3075.
- (5) Mattheus, C. C.; Baas, J.; Meetsma, A.; Boer, J. L. d.; Kloc, C.; Siegrist, T.; Palstra, T. T. M., A 2:1 cocrystal of 6,13-dihydropentacene and pentacene. *Acta Crystallogr., Sect. E*, **2002**, *58*, o1229-o1231.
- (6) Rogers, C.; Chen, C.; Pedramrazi, Z.; Omrani, A. A.; Tsai, H.-Z.; Jung, H. S.; Lin, S.; Crommie, M. F.; Fischer, F. R., Closing the Nanographene Gap: Surface-Assisted Synthesis of Peripentacene from 6,6'-Bipentacene Precursors. *Angew. Chem., Int. Ed.*, **2015**, *54*, 15143-15146.
- (7) Heya, A.; Matsuo, N., Guidelines for bottom-up approach of nanocarbon film formation from pentacene using heated tungsten on quartz substrate without metal catalyst. **2018**, *57*, 04FL03.
- (8) Northrop, B. H.; Norton, J. E.; Houk, K. N., On the Mechanism of Peripentacene Formation from Pentacene: Computational Studies of a Prototype for Graphene Formation from Smaller Acenes. *J. Am. Chem. Soc.*, **2007**, *129*, 6536-6546.
- (9) Zöphel, L.; Berger, R.; Gao, P.; Enkelmann, V.; Baumgarten, M.; Wagner, M.; Müllen, K., Toward the peri-Pentacene Framework. *Chem. - Eur. J.*, **2013**, *19*, 17821-17826.
- (10) Sarobe, M.; Jenneskens, L. W.; Wiersum, U. E., Thermolysis of benzo[c]phenanthrene: Conversion of an alternant C₁₈H₁₂ PAH into Non-alternant C₁₈H₁₀ PAHs. *Tetrahedron Lett.*, **1996**, *37*, 1121-1122.
- (11) Zeis, R.; Besnard, C.; Siegrist, T.; Schlockermann, C.; Chi, X.; Kloc, C., Field Effect Studies on Rubrene and Impurities of Rubrene. *Chem. Mater.*, **2006**, *18*, 244-248.
- (12) Lewis, I. C.; Edstrom, T., Thermal Reactivity of Polynuclear Aromatic Hydrocarbons¹. *Org. Chem.*, **1963**, *28*, 2050-2057.
- (13) Field, L. D.; Sternhell, S.; Wilton, H. V., Mechanochemistry of some hydrocarbons. *Tetrahedron*, **1997**, *53*, 4051-4062.
- (14) Ishii, Y.; Sakashita, T.; Kawasaki, S.; Kato, H.; Takatori, M., Fusing Treatment of Pentacenes: Toward Giant Graphene-Like Molecule. *Mater. Express*, **2011**, *1*, 36-42.
- (15) Mattheus, C. C.; Dros, A. B.; Baas, J.; Meetsma, A.; Boer, J. L. d.; Palstra, T. T. M., Polymorphism in pentacene. *Acta Crystallogr. C*, **2001**, *57*, 939-941.
- (16) Siegrist, T.; Besnard, C.; Haas, S.; Schiltz, M.; Pattison, P.; Chernyshov, D.; Batlogg, B.; Kloc, C., A Polymorph Lost and Found: The High-Temperature Crystal Structure of Pentacene. *Adv. Mater.*, **2007**, *19*, 2079-2082.
- (17) Siegrist, T.; Kloc, C.; Schön, J. H.; Batlogg, B.; Haddon, R. C.; Berg, S.; Thomas, G. A., Enhanced Physical Properties in a Pentacene Polymorph. *Angew. Chem. Int. Ed.*, **2001**, *40*, 1732-1736.
- (18) Holmes, D.; Kumaraswamy, S.; Matzger, A. J.; Vollhardt, K. P. C., On the Nature of Nonplanarity in the [N]Phenylenes. *Chem. Eur. J.*, **1999**, *5*, 3399-3412.
- (19) Ehrenberg, M., The crystal structure of di-para-anthracene. *Acta Crystallogr.*, **1966**, *20*, 177-182.
- (20) Gaultier, J.; Hauw, C.; Desvergne, J. P.; Lapouyade, R., *Cryst. Str. Commun.*, **1975**, *4*.

- 1
2
3 (21) Berg, O.; Chronister, E. L.; Yamashita, T.; Scott, G. W.; Sweet, R. M.; Calabrese, J., s-Dipentacene:
4 Structure, Spectroscopy, and Temperature- and Pressure-Dependent Photochemistry. *J. Phys. Chem.*
5 *A*, **1999**, *103*, 2451-2459.
6 (22) Sinnokrot, M. O.; Sherrill, C. D., Highly Accurate Coupled Cluster Potential Energy Curves for the
7 Benzene Dimer: Sandwich, T-Shaped, and Parallel-Displaced Configurations. *J. Phys. Chem. A*, **2004**,
8 *108*, 10200-10207.
9 (23) Nemanich, R. J.; Solin, S. A., First- and second-order Raman scattering from finite-size crystals of
10 graphite. *Phys. Rev. B*, **1979**, *20*, 392-401.
11 (24) Ferrari, A. C.; Robertson, J., Interpretation of Raman spectra of disordered and amorphous
12 carbon. *Phys. Rev. B*, **2000**, *61*, 14095-14107.
13 (25) Ferrari, A. C.; Meyer, J. C.; Scardaci, V.; Casiraghi, C.; Lazzeri, M.; Mauri, F.; Piscanec, S.; Jiang, D.;
14 Novoselov, K. S.; Roth, S.; Geim, A. K., Raman Spectrum of Graphene and Graphene Layers. *Phys. Rev.*
15 *Let.*, **2006**, *97*, 187401.
16 (26) Ferrari, A. C., Raman spectroscopy of graphene and graphite: Disorder, electron-phonon
17 coupling, doping and nonadiabatic effects. *Solid State Commun.*, **2007**, *143*, 47-57.
18 (27) Malard, L. M.; Pimenta, M. A.; Dresselhaus, G.; Dresselhaus, M. S., Raman spectroscopy in
19 graphene. *Phys. Rep.*, **2009**, *473*, 51-87.
20 (28) Martins Ferreira, E. H.; Moutinho, M. V. O.; Stavale, F.; Lucchese, M. M.; Capaz, R. B.; Achete, C.
21 A.; Jorio, A., Evolution of the Raman spectra from single-, few-, and many-layer graphene with
22 increasing disorder. *Phys. Rev. B*, **2010**, *82*, 125429.
23 (29) Cançado, L. G.; Jorio, A.; Ferreira, E. H. M.; Stavale, F.; Achete, C. A.; Capaz, R. B.; Moutinho, M. V.
24 O.; Lombardo, A.; Kulmala, T. S.; Ferrari, A. C., Quantifying Defects in Graphene via Raman
25 Spectroscopy at Different Excitation Energies. *Nano Lett.*, **2011**, *11*, 3190-3196.
26 (30) Verzhbitskiy, I. A.; Corato, M. D.; Ruini, A.; Molinari, E.; Narita, A.; Hu, Y.; Schwab, M. G.; Bruna,
27 M.; Yoon, D.; Milana, S.; Feng, X.; Müllen, K.; Ferrari, A. C.; Casiraghi, C.; Prezzi, D., Raman Fingerprints
28 of Atomically Precise Graphene Nanoribbons. *Nano Lett.*, **2016**, *16*, 3442-3447.
29 (31) Yi, M.; Shen, Z., A review on mechanical exfoliation for the scalable production of graphene. *J.*
30 *Mater. Chem. A*, **2015**, *3*, 11700-11715.
31 (32) Nagano, M.; Hasegawa, T.; Myoujin, N.; Yamaguchi, J.; Itaka, K.; Fukumoto, H.; Yamamoto, T.;
32 Koinuma, H., The First Observation of 1 H-NMR Spectrum of Pentacene. *Jpn. J. Appl. Phys.*, **2004**, *43*,
33 L315.
34 (33) Caldwell, W. E.; Odom, J. D.; Williams, D. F., Glass-Sample-Tube Breaker. **1983**, *55*, 1175-1176.
35
36
37
38
39
40
41
42
43
44
45
46
47
48
49
50
51
52
53
54
55
56
57
58
59
60

TOC Graphical abstract

